Synaptic signal transduction aided by noise in a dynamical saturating model

François Chapeau-Blondeau*
Laboratoire d'Ingénierie des Systèmes Automatisés (LISA), Université d'Angers, 62 Avenue Notre Dame du Lac, 49000 Angers, France

Fabing Duan†
Institute of Complexity Science, Department of Automation Engineering, Qingdao University, Qingdao 266071, People's Republic of China

Derek Abbott‡
Centre for Biomedical Engineering (CBME) and School of Electrical and Electronic Engineering, The University of Adelaide, South Australia 5005, Australia

(Received 15 September 2009; published 22 February 2010)

A generic dynamical model with saturation for neural signal transduction at the synaptic stage is presented. Analysis of this model of a synaptic pathway demonstrates its ability to give rise to stochastic resonance or improvement by noise, at this stage of signal transmission. Beyond the case of the intrinsic threshold nonlinearity of the neuron response, the results extend the feasibility of stochastic resonance to neural saturating dynamics at the synaptic stage. The present results also constitute the exposition of a new type of nonlinear (saturating) dynamics capable of stochastic resonance.

DOI: 10.1103/PhysRevE.81.021124 PACS number(s): 05.40.−a, 05.45.−a, 87.10.−e

I. INTRODUCTION

Neural systems perform very efficient signal and information processing [1–3]. They implement, as a basis, complex dynamics that very often involve nonlinear processes [1–3]. Also, neural systems commonly have to operate in environments containing noise, either of external or internal origins [4–9]. It is now known that nonlinear systems in the presence of noise can sometimes give rise to a cooperative effect where the noise can play a part to improve signal processing. This type of cooperative nonlinear effect is often called stochastic resonance [10–17]. Stochastic resonance has mainly been observed and analyzed in nonlinear systems with potential barriers [10–12] or thresholds [14–22]. In these conditions, noise essentially assists a usually small signal in driving transitions of the system across thresholds or barriers in a more efficient way. The possibility of this type of stochastic resonance has been identified in neural processes [4–8,11–18,20–23]. In this context, an essential nonlinearity is the threshold nonlinearity in the response of the neuron, and many studies of stochastic resonance have been proposed for this case [13–18,20–23]. Also, interesting aspects for neurons assembled in networks are analyzed in [24–32].

However, some studies have established another possibility for stochastic resonance in barrier-free or threshold-free systems [33–35]. Also more recently, it has been recognized that stochastic resonance can also occur in threshold-free nonlinearities exhibiting saturation [36–40]. Improvement by noise was reported with static or memoryless saturating nonlinearities in [36–38]. Such a result was applied to a model for the saturation of the output firing activity of a neuron that was shown to exhibit stochastic resonance [41,42]. Very recently, Refs. [39,40] reported stochastic resonance in dynamic systems with saturation, yet with no reference to neural processes. In the present paper here, we argue that an essentially saturating dynamics can also be found in neural processes at the synaptic stage. Then we demonstrate that this saturating dynamics can elicit an effect of stochastic resonance or improvement by noise of synaptic signal transduction. The present results are of significance both for the analysis and modeling of neural processes, and also for the range and analysis of nonlinearities capable of stochastic resonance.

II. SATURATING DYNAMICS IN SYNAPTIC TRANSMISSION

An essential nonlinearity in neural signal transmission is the threshold nonlinearity in the response of a single neuron [13–18,20–23]. Another type of nonlinearity is also present at several stages of neural signal transmission, which is essentially a saturating nonlinearity [1,2,23,43].

For instance, in synaptic transmission at the presynaptic stage, an incoming signal triggers the release of neurotransmitter molecules in the synaptic cleft, of quantity $q(t)$. The evolution of $q(t)$ is returned to zero by the clearance processes in the cleft. The evolution of $q(t)$ also includes a growth mechanism related to the intensity of the incoming presynaptic signal. However, this growth of $q(t)$ draws upon a finite population of neurotransmitter vesicles. This causes, in case of a strong sustained presynaptic activity, a saturation in the growth of $q(t)$ as the population of vesicles exhausts. A possible model for this dynamics is as follows:

$$\frac{dq}{dt} = -\frac{q(t)}{\tau_q} + [q_{\text{sat}} - q(t)]\alpha_q E(t). \tag{1}$$

In Eq. (1), the input $E(t)$ is a non-negative quantity representing the firing activity down the presynaptic axon, as for

*chapeau@univ-angers.fr
†fabing.duan@gmail.com
‡dabbott@eleceng.adelaide.edu.au

instance a short-term average of action potentials or a firing rate. Also in Eq. (1), the relaxation term $-q(t)/\tau_q$, which drives $q(t)$ to zero, represents the clearance processes with time constant τ_q. The growth term $[q_{\rm sat}-q(t)]\alpha_q E(t)$ is proportional to the presynaptic activity $E(t)$. However, a proportionality factor with the form $[q_{\rm sat}-q(t)]\alpha_q$ gradually extinguishes the action of the driving input $E(t)$ as $q(t)$ approaches the saturation level $q_{\rm sat}$, thus preventing $q(t)$ from growing above $q_{\rm sat}$. Here, α_q is a positive dimensionless constant measuring the efficiency of the conversion process of $E(t)$ into $q(t)$. Equation (1) therefore describes the nonlinear dynamics of a saturating type.

A similar picture exists at the postsynaptic stage. The neurotransmitter molecules trigger the gating of ion channels in the membrane of the postsynaptic neuron. The number of open postsynaptic channels we denote as $n(t)$. The evolution of $n(t)$ is also returned to zero as a consequence of the clearing of the neurotransmitter out of the cleft. The evolution of $n(t)$ also includes a growth mechanism related to the quantity $q(t)$ of neurotransmitter present in the cleft. However, this growth of $n(t)$ draws upon a finite population of postsynaptic channels. This causes, in the case of a large sustained $q(t)$, a saturation in the growth of $n(t)$ as all channels become recruited. A possible model for this dynamics is

$$\frac{dn}{dt} = -\frac{n(t)}{\tau_n} + [n_{\rm sat} - n(t)]\alpha_n q(t). \tag{2}$$

The terms in Eq. (2) have a similar interpretation to those in Eq. (1). Equation (2) again represents nonlinear dynamics of a saturating type, which prevents $n(t)$ from evolving above the saturation level $n_{\rm sat}$.

Each open ion channel of the postsynaptic membrane can be assigned a fixed electric conductance g. The total conductance $G(t)=gn(t)$ of the postsynaptic membrane at this synapse, is therefore also governed by saturating dynamics as in Eq. (2). The change of membrane conductance $G(t)$ at this synapse induces a somatic current $I(t)$ that directly drives the evolution of the membrane potential $V(t)$ of the postsynaptic neuron, which fires an output spike each time $V(t)$ reaches the firing threshold $V_{\rm th}$. The driving current $I(t)$ is expressed as $I(t)=G(t)[V_{\rm rev}-V(t)]$, where $V_{\rm rev}$ is the reversal potential of the synapse ($V_{\rm rev}$ is above the neuron resting potential $V_{\rm rest}$ for an excitatory synapse and below for an inhibitory synapse) [1,2,43]. For many synapses $V_{\rm rev}$ is such that the excursion of $V(t)$, which takes place around the resting potential $V_{\rm rest}$ and at most up to the firing threshold $V_{\rm th}$, is small in relation to the distance $[V_{\rm rev}-V(t)]$; this allows one to approximate the synaptic current as $I(t)=G(t)[V_{\rm rev}-V_{\rm rest}]$. With this fixed proportionality constant $[V_{\rm rev}-V_{\rm rest}]$, it turns out that the synaptic current $I(t)$ is also governed by the saturating dynamics in Eq. (2). With several synapses on the same postsynaptic neuron, the currents $I(t)$ contributed by each synapse simply add up to drive the membrane potential.

The transmission from the presynaptic activity $E(t)$ to the postsynaptic current $I(t)$ directly driving the neuron is therefore essentially governed by saturating dynamics according to Eqs. (1) and (2). From $E(t)$ to $I(t)$ the cascaded dynamics of Eqs. (1) and (2) can be considered in a regime where only one of the two saturations operates, while the other dynamics evolves sufficiently below its saturation to be purely linear. This regime still provides a useful view on the impact of saturation in signal transmission, yet with a simpler approach. We are thus led to study dynamics of the generic form

$$\frac{dI}{dt} = -\frac{I(t)}{\tau} + [I_{\rm sat} - I(t)]\alpha E(t). \tag{3}$$

In this way, Eq. (3) can be viewed as a model for one stage of the transmission either by Eq. (1) or by Eq. (2), or for the two-stage cascaded transmission when only one of the two saturations dominates, while the other dynamics is sufficiently faster and remains below its saturation in a quasilinear regime.

In the absence of noise, the solution to Eq. (3) with initial condition $I(t_0)=I_0$ reads for $t \geq t_0$

$$I(t) = \left\{ I_0 + I_{\rm sat}\int_{t_0}^{t} \alpha E(t'')\exp\left[\frac{t''-t_0}{\tau} + \int_{t_0}^{t''} \alpha E(t')dt'\right]dt''\right\}\exp\left[-\frac{t-t_0}{\tau} - \int_{t_0}^{t} \alpha E(t')dt'\right]. \tag{4}$$

We will now investigate the possibility of stochastic resonance or improvement by noise in synaptic signal transmission by the generic saturating nonlinear dynamics of Eq. (3). A comparable but distinct saturating dynamic was shown in [39,40] to exhibit stochastic resonance, but with no reference to the neural context we examine here.

III. INPUT-OUTPUT CORRELATION MEASURE

Based on the neural interpretation of Eqs. (1)–(3), the input signal $E(t)$ in Eq. (3) is non-negative, and represents the presynaptic activity at the input of the transmission pathway. The input signal $E(t)$ of Eq. (3) is taken as the superposition $E(t)=s(t)+\xi(t)$ of a deterministic aperiodic waveform $s(t)$ and noise $\xi(t)$. Both components $s(t)$ and $\xi(t)$ are separately formed with the same neural substrate as $E(t)$, and share the same nature of non-negative signals that describe presynaptic activity, be it a spontaneous random activity for $\xi(t)$ or a coherent activity for $s(t)$.

Accordingly, $\xi(t)$ is modeled as non-negative white noise, with a probability density function $f_\xi(u)$ for which various standard forms will be considered. For the non-negative $\xi(t)$, we will consider the uniform probability density

$$f_\xi(u) = \begin{cases} 1/b, & 0 < u < b \\ 0, & \text{otherwise}, \end{cases} \tag{5}$$

with mean $b/2$, variance $b^2/12$, and root mean squared (rms) amplitude $\xi_{\rm rms}=b/\sqrt{3}$. We will also consider the Gamma probability density of order $a \geq 1$, as

$$f_\xi(u) = \begin{cases} \dfrac{1}{b^a\Gamma(a)}u^{a-1}\exp\left(-\dfrac{u}{b}\right), & u \geq 0 \\ 0, & u < 0, \end{cases} \tag{6}$$

where $\Gamma(a)=\int_0^\infty x^{a-1}\exp(-x)dx$, the mean value of $\xi(t)$ being ab, its variance ab^2, and its rms amplitude $\xi_{\rm rms}=b\sqrt{a^2+a}$.

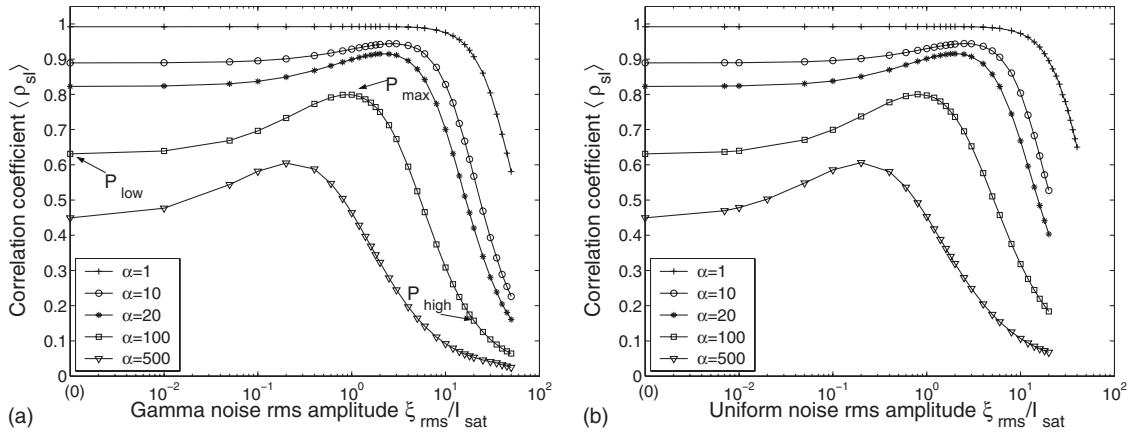

FIG. 1. Ensemble-averaged correlation coefficient $\langle \rho_{sI} \rangle$ between input $s(t)$ and output $I(t)$, as a function of the noise rms amplitude $\xi_{\rm rms}$, at different values of the gain parameter α in Eq. (3). The input signal $s(t)$ from Eq. (9) is with $T_s = 10^3 \tau$, $A_1 = 5I_{\rm sat}$, $A_2 = 3I_{\rm sat}$, and $A_3 = 2I_{\rm sat}$ as represented in Fig. 2(a). The noise $\xi(t)$ is (a) Gamma of order $a=2$, (b) uniform. Each point was averaged over 1000 trials. For simplicity, we represent the origin tick 10^{-3} of the logarithmic x axis as zero, and $\xi_{\rm rms}$ increases from zero actually.

With a deterministic aperiodic coherent input $s(t)$, a useful input-output measure of similarity, frequently used in stochastic resonance studies, is the correlation coefficient [15,16] of the input $s(t)$ with the output $I(t)$, which we define as

$$\rho_{sI} = \max_{\tau_d} \frac{\overline{[s(t) - \overline{s(t)}][I(t+\tau_d) - \overline{I(t+\tau_d)}]}}{\left\{ \overline{[s(t) - \overline{s(t)}]^2} \, \overline{[I(t+\tau_d) - \overline{I(t+\tau_d)}]^2} \right\}^{1/2}} \tag{7}$$

$$= \max_{\tau_d} \frac{\overline{s(t) I(t+\tau_d)} - \overline{s(t)}\,\overline{I(t+\tau_d)}}{\left\{ \overline{[s(t) - \overline{s(t)}]^2} \, \overline{[I(t+\tau_d) - \overline{I(t+\tau_d)}]^2} \right\}^{1/2}}, \tag{8}$$

where the overbar denotes a temporal average, and the maximum is taken over the time lag $\tau_d \geq 0$. This time lag τ_d is introduced in order to take into account a possible propagation delay induced by the dynamic system of Eq. (3), and the maximum corresponds to finding the optimal delay entailing the best match between $s(t)$ and $I(t+\tau_d)$.

IV. STOCHASTIC RESONANCE IN SATURATING DYNAMICS

When the noise input $\xi(t)$ is absent, Eq. (4) represents the system output exactly. In the noise-free case, the correlation coefficient ρ_{sI} between $I(t)$ and $s(t)$ can then be computed directly according to Eq. (8). When the noise $\xi(t)$ is present at the input, the system response $I(t)$ will be simulated numerically, and an ensemble averaging of the correlation coefficient ρ_{sI} will be performed over independent realizations of the noise to yield $\langle \rho_{sI} \rangle$, following the common practice in stochastic resonance studies [15,16]. In numerical simulations of Eq. (3), the Euler-Maruyama method is used [44], with a sampling time step Δt much less than the time constant τ and the signal duration T_s, and which is fixed at $\Delta t = 0.1\tau$ throughout.

The coherent input signal $s(t)$ is defined over $t \in [0, T_s]$ as

$$s(t) = A_1 \sin(\pi t/T_s) + A_2 \sin(3\pi t/T_s) + A_3 \sin(7\pi t/T_s), \tag{9}$$

with $s(t)$ being zero outside $[0, T_s]$. An example of the waveform $s(t)$ of Eq. (9) is depicted in Fig. 2(a). The purpose of Eq. (9) is to have a non-negative signal $s(t)$, which carries some distinctive features in the upper part of the waveform that can suffer from saturation in transmission by Eq. (3).

A. Influence of the gain parameter α

The transmission by Eq. (3) of $s(t)$ added to the noise $\xi(t)$ is then studied. The influence of the rms amplitude $\xi_{\rm rms}$ of the noise is examined, for different values of the gain parameter α. Figure 1 shows the ensemble-averaged correlation coefficient $\langle \rho_{sI} \rangle$ between the input $s(t)$ and the output $I(t)$.

The main feature visible in Fig. 1 is that, as the noise level $\xi_{\rm rms}$ increases, the input-output correlation coefficient $\langle \rho_{sI} \rangle$, measuring the efficacy of signal transmission, can sometimes experience a nonmonotonic evolution, depending on the gain parameter α. For small gain $\alpha = 1$ in Fig. 1, the system of Eq. (3) operates in a quasilinear regime, away from saturation. In this case, the correlation coefficient $\langle \rho_{sI} \rangle$ is at a high value close to unity at zero noise $\xi_{\rm rms} = 0$, and $\langle \rho_{sI} \rangle$ degrades (decreases) as the noise level $\xi_{\rm rms}$ increases. The noise only acts as a nuisance in this quasilinear regime.

For a larger gain parameter α in Fig. 1, the system of Eq. (3) leads to the operation in the saturation region. In this case, the output response $I(t)$ gets distorted by the saturation, and the correlation coefficient $\langle \rho_{sI} \rangle$ is degraded at zero noise $\xi_{\rm rms} = 0$ because of this distortion. However, in this nonlinear saturating regime, as the noise level $\xi_{\rm rms}$ is raised above zero, Fig. 1 reveals the possibility of an improvement of $\langle \rho_{sI} \rangle$. The correlation coefficient $\langle \rho_{sI} \rangle$, measuring the efficacy of transmission, culminates at a maximum for a nonvanishing level of noise. This is an effect of stochastic resonance or improvement by noise, which is shown possible in the neural saturating dynamics of Eq. (3).

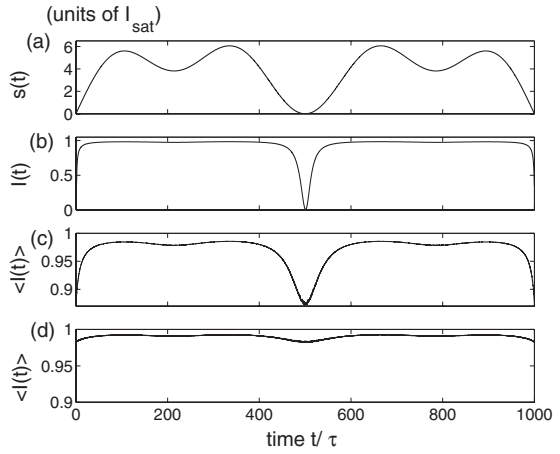

FIG. 2. (a) Input signal $s(t)$ from Eq. (9) as used in Fig. 1. (b) System output $I(t)$ calculated from Eq. (4) at the Gamma noise rms amplitude $\xi_{\rm rms}=0$. Ensemble average of system output $\langle I(t)\rangle$ at the Gamma noise rms amplitude of (c) $\xi_{\rm rms}=1.05I_{\rm sat}$ and (d) $\xi_{\rm rms}=12I_{\rm sat}$. Respectively, (b), (c), and (d) correspond to the three points $P_{\rm low}$, $P_{\rm max}$, and $P_{\rm high}$ in Fig. 1(a). Other parameters are the same as in Fig. 1.

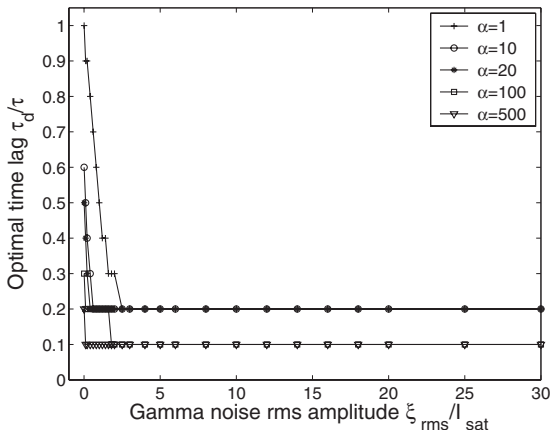

FIG. 3. Optimal time lag τ_d in Eq. (8) versus Gamma noise rms amplitude $\xi_{\rm rms}$ corresponding to Fig. 1(a). Other parameters are the same as in Fig. 1.

Beyond the feasibility of the stochastic resonance effect, Fig. 1 also shows more detailed modalities: As the gain parameter α is further increased, the saturation in Eq. (3) gets more pronounced, as well as the magnitude of the improvement of $\langle\rho_{sI}\rangle$, while the optimal noise level maximizing $\langle\rho_{sI}\rangle$ gets closer to zero, in the conditions of Fig. 1. We also observe that the feasibility of the stochastic resonance effect is not critically dependent on the type of the noise $\xi(t)$. The effect is preserved for Gamma or uniform noise, as illustrated in Figs. 1(a) and 1(b), respectively.

To further illustrate the constructive role of noise, three points $P_{\rm low}$, $P_{\rm max}$, and $P_{\rm high}$ are selected in Fig. 1(a) from the curve of $\langle\rho_{sI}\rangle$ at the gain parameter $\alpha=100$, corresponding to the Gamma noise rms amplitudes $\xi_{\rm rms}=0$, $1.05I_{\rm sat}$, and $12I_{\rm sat}$, respectively. The input signal $s(t)$ of Eq. (9) is plotted in Fig. 2(a). The system output $I(t)$, at the noise rms amplitude $\xi_{\rm rms}=0$, is deduced from Eq. (4) and plotted in Fig. 2(b). Also superimposed in Fig. 2(b) is the same signal $I(t)$ yet computed by numerical simulation of Eq. (3). This gives us the occasion, with the conditions of Fig. 2(b), to verify that our numerical integration scheme for Eq. (3) perfectly matches the analytical solution of Eq. (4).

It is seen in Fig. 2(b) that the system response $I(t)$, relative to the input signal waveform of $s(t)$, is mainly compressed by the saturation of the dynamical system of Eq. (3), and displays two relatively flat bumps separated by a very narrow valley. By comparison with the input signal $s(t)$ of Fig. 2(a), $I(t)$ in Fig. 2(b) loses the high-amplitude variations of the top bumps, and compresses the wide valley of $s(t)$ into a narrow one. Thus, the correlation coefficient between the input $s(t)$ and the output $I(t)$ yields $\langle\rho_{sI}\rangle=0.6311$ at the point $P_{\rm low}$. Next, when the noise rms amplitude is increased to $\xi_{\rm rms}=1.05I_{\rm sat}$, it is observed in Fig. 2(c) that the waveform of $I(t)$ better matches the input signal $s(t)$ and achieves the maximum degree of similarity with $s(t)$. The action of noise raises and enlarges the valley of the system output $I(t)$, resulting in a more similar waveform to the input signal $s(t)$. Accordingly, the correlation coefficient between the input $s(t)$ and the output $I(t)$ reaches its maximum $\langle\rho_{sI}\rangle=0.7991$ at the point $P_{\rm max}$ of Fig. 1(a). Next, when the noise rms amplitude is further increased to $\xi_{\rm rms}=12I_{\rm sat}$ at the point $P_{\rm high}$, the amount of noise becomes critical. This strongly degrades the output $I(t)$ that largely loses its similarity with the input $s(t)$, as visible in Fig. 2(d) where the response is dominated by saturation. In this situation, the correlation coefficient between the input $s(t)$ and the output $I(t)$ drops to $\langle\rho_{sI}\rangle=0.2609$. An interpretation of the sequence of Fig. 2 is that a suitable amount of added noise has the ability, on average, to pull the output $I(t)$ away from the strong saturation regime and back into the more linear part of the response. This produces an output $I(t)$ more similar to the input $s(t)$ thanks to an appropriate amount of added noise. This mode of action of the noise illustrated in Fig. 2 can be interpreted as a form of noise-induced linearization, as analyzed in [45,46] in other different nonlinear systems. Nevertheless, stochastic resonance appears as a complex phenomenon that contains more than noise-induced linearization, since in nonlinear systems stochastic resonance can produce effects that no linear system can achieve, for instance signal-to-noise ratio gains above unity [47–49], although this aspect is not in itself addressed in the present study.

Additionally, we plot in Fig. 3 the variation of the optimal time lag τ_d in Eq. (8) versus the noise rms amplitude $\xi_{\rm rms}$. Upon increasing the noise level $\xi_{\rm rms}$, as observed in Fig. 3, the optimal time lag τ_d is rapidly reduced, this occurring generally, for different values of the gain α. This manifests another effect of the noise, which is to reduce the system response time or propagation delay of the coherent input $s(t)$ across the dynamical system. A similar action of the noise to accelerate the temporal response of the saturating dynamics of Eq. (3) was also observed in the two-state bistable dynamics constituting a very classic stochastic resonator [50].

B. Influence of the signal duration T_s

In Fig. 4, we plot the ensemble-averaged correlation coefficient $\langle\rho_{sI}\rangle$ as a function of the noise rms amplitude $\xi_{\rm rms}$

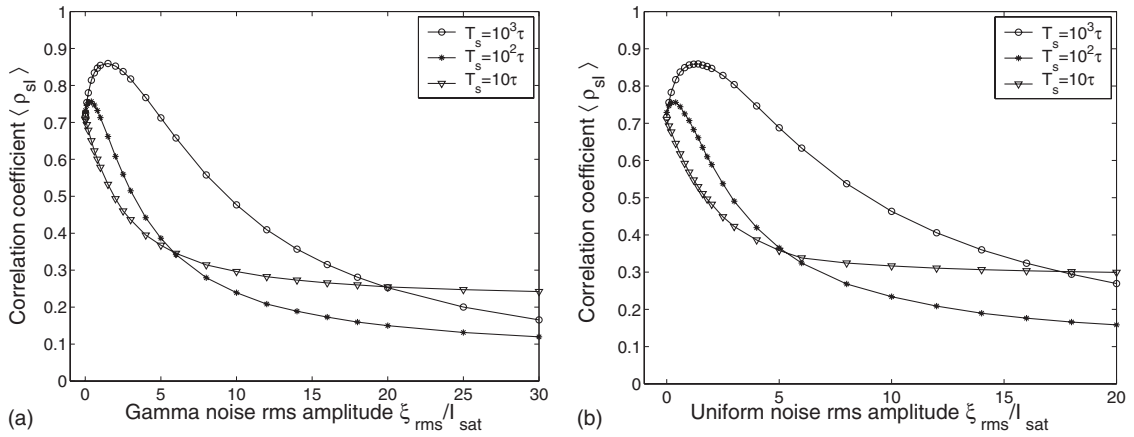

FIG. 4. Ensemble-averaged correlation coefficient $\langle \rho_{sI} \rangle$ between input $s(t)$ and output $I(t)$, as a function of the noise rms amplitude ξ_{rms}, at $\alpha=50$ in Eq. (3), for different durations T_s of the input signal $s(t)$ of Eq. (9) with $A_1=5I_{\text{sat}}$, $A_2=3I_{\text{sat}}$ and $A_3=2I_{\text{sat}}$. The noise $\xi(t)$ is (a) Gamma of order $a=2$, (b) uniform. Each point was averaged over 1000 trials.

for different durations T_s of the coherent input $s(t)$. Here, the gain parameter $\alpha=50$ in Eq. (3) is fixed, which makes the system state mainly operate in a moderate saturating region. At large duration $T_s=10^3\tau$, the increase of the noise level improves the system response to the input signal $s(t)$, yielding a marked resonant behavior of $\langle \rho_{sI} \rangle$, as shown in Fig. 4. As the time duration T_s decreases to $10^2\tau$, the resonant evolution of $\langle \rho_{sI} \rangle$ is gradually reduced. At $T_s=10^2\tau$ in Fig. 4, the resonance peak of $\langle \rho_{sI} \rangle$ is relatively low, and the resonance region of the noise rms amplitude ξ_{rms} occurs closer to zero. When the duration T_s is further reduced to 10τ in Fig. 4, the stochastic resonance effect disappears. The noise returns to its traditional role as a nuisance, with the correlation coefficient $\langle \rho_{sI} \rangle$ decreasing monotonically as ξ_{rms} grows. The nonlinear saturating dynamics of Eq. (3) incorporates an intrinsic time constant τ, and the present analysis shows that the duration T_s of an aperiodic input signal $s(t)$ has to be sufficiently large compared to τ, in order for $s(t)$ to be able to take benefit from a constructive action of noise to reduce negative effects of saturation, which can occur in its transmission by Eq. (3). In this situation, the optimal time lags τ_d in Eq. (8) for different durations T_s of the coherent input $s(t)$ are in the interval of $[0.1,0.4]\tau$ (not shown here). As the duration T_s decreases from $10^3\tau$ to 10τ, the same waveform's variations of $s(t)$, as shown in Fig. 2(a), will be restricted within the reduced duration T_s. The system response $I(t)$ barely has time to catch the change of the coherent input $s(t)$ that is compressed by the saturating region of Eq. (3), even by the help of noise at an optimal time lag τ_d for computing the best match between $s(t)$ and $I(t+\tau_d)$.

V. CONCLUSION

In this paper, we studied a generic nonlinear dynamical system with saturation, which offers a model for neural signal transmission at the synaptic stage. We especially studied conditions where the gain α of the synaptic pathway is large, or equivalently where the applied input signal $s(t)$ is large. In such conditions, saturation naturally occurs in the transmission, producing nonlinear distortion of the transmitted signal. In this regime, we established the possibility of a stochastic resonance effect, or an effect of improvement by noise of the signal transmission under saturation. Conditions exist where an optimal nonzero amount of noise maximizes the efficacy of transmission as measured by the input-output correlation. The effect of noise is to reduce the nonlinear saturating distortion experienced by the signal, and to restore conditions closer to linear transmission. The beneficial action of the added noise can be viewed as realizing, on average, a displacement of the operating zone of the transmission system, which is taken away from the saturating region to be pulled back toward its linear region, resulting in a better input-output correlation. The nonlinear saturating dynamics of Eq. (3) is thus established as a new dynamical system capable of stochastic resonance or improvement by noise.

It is interesting to note that, compared to more traditional threshold or potential-barrier dynamics, the improvement by noise in the saturating dynamics of Eq. (3) takes place in more demanding conditions. The noise $\xi(t)$ here associated with Eq. (3), is a non-negative noise, which fluctuates around a nonzero mean $\langle \xi(t) \rangle$. This non-negative character of the noise $\xi(t)$ arises from the neural interpretation of the dynamics of Eq. (3), where the noise $\xi(t)$ describes fluctuations of inherently non-negative quantities (such as rate of spontaneous firing or number of released neurotransmitter vesicles). The level of the non-negative noise $\xi(t)$ is increased here by increasing the parameter b in Eqs. (5) and (6). This in fact produces both an increase in the standard deviation and in the mean of $\xi(t)$, and this is summarized by the increase of the rms amplitude ξ_{rms} with its beneficial outcome observed in Figs. 1–4. An increase in the positive mean $\langle \xi(t) \rangle$ alone has a detrimental impact on signal transmission, because it acts in the direction of accentuating the saturation. So as the noise is raised, the fluctuating part of the noise has reduced benefit, because it also has to compensate the unfavorable action of the increasing mean $\langle \xi(t) \rangle$. By contrast, in traditional stochastic resonance, with threshold or potential-barrier nonlinearities, the noise usually keeps a zero mean, and there is no antagonist action of an increasing unfavorable noise mean to compensate, so the task of the noisy fluctuation is in this respect easier. This reveals an especially pow-

erful capability of the noisy fluctuation associated with the saturating nonlinearity of Eq. (3) to induce the benefit improving signal transmission. This is a contribution of the present study, in the area of stochastic resonance, to expose a new type of nonlinear dynamical system that is shown to give rise to improvement by noise.

Now, in the area of neural modeling, the main characteristic of the present study is that it concentrates on neural signal transmission at the synaptic stage. The model essentially describes the synaptic pathway from the firing activity down a presynaptic axon to the synaptic current contributed into a postsynaptic neuron. We have demonstrated that such a synaptic pathway incorporates a saturating nonlinearity and that this nonlinearity lends itself to stochastic resonance or improvement by noise of signal transmission. Our demonstration is accomplished here based on a simple yet plausible theoretical model of the synaptic pathway. Beyond this theoretical proof of feasibility, further studies will be necessary to establish whether real neural processes in *in vivo* conditions do exploit this possibility in actuality. This could require more refined modeling, but also essentially experimental studies.

On the modeling side, the present treatment of Eq. (3) describes transmission through one single synaptic pathway. This is a basic stage where improvement by noise is already shown possible here. One could next consider several synaptic pathways, modeled through Eq. (3), each receiving an excitatory or an inhibitory character as explained in Sec. II, and converging upon a same postsynaptic neuron. More elaborate dynamics could be accessible in this way, for examining how the beneficial action of noise evolves, upon transduction through multiple synaptic pathways.

Subsequent to the saturating dynamics of the synaptic pathway, the threshold dynamics of the neuronal response has been more often considered in relation to stochastic resonance, and as such it is not part of the present study. This leads to a natural extension for the present results, to combine the saturating dynamics of the synaptic stage to the threshold dynamics of the neuronal stage. This combination offers a more detailed description of neural dynamics, and allows one to investigate the richer capabilities of noise-improved neural signal transmission, taking into account the existence of both saturation and threshold in the processes. Further, at a higher level of organization, association of such neural units with saturation and threshold into networks could also give rise to still richer possibilities of stochastic resonance in neural signal transmission and processing. In this respect, the parallel arrays considered in [27,28,30,31,42] could be investigated with the threshold and saturating neural units, to analyze how their capabilities for stochastic resonance evolve with such richer constituents. In this way, the present results revealing stochastic resonance in the saturating behavior of the synapse can contribute, at different levels, to the investigation of the complex and possibly useful role of noise in neuronal dynamics for signal and information processing in the nervous system.

ACKNOWLEDGMENTS

This work was sponsored by NSFC (Grant No. 60602040) and Taishan Scholar CPSP. Funding from the Australian Research Council (ARC) is gratefully acknowledged.

[1] C. Koch and I. Segev, *Methods in Neuronal Modeling* (MIT, Cambridge, MA, 1989).
[2] P. Dayan and L. F. Abbott, *Theoretical Neuroscience: Computational and Mathematical Modeling of Neural Systems* (MIT, Cambridge, MA, 2001).
[3] A. V. Holden, Nature (London) **428**, 382 (2004).
[4] J. K. Douglass, L. Wilkens, E. Pantazelou, and F. Moss, Nature (London) **365**, 337 (1993).
[5] H. A. Braun, H. Wissing, K. Schäfer, and M. C. Hirsch, Nature (London) **367**, 270 (1994).
[6] D. F. Russell, L. A. Wilkens, and F. Moss, Nature (London) **402**, 291 (1999).
[7] A. A. Faisal, L. P. J. Selen, and D. M. Wolpert, Nat. Rev. Neurosci. **9**, 292 (2008).
[8] J. M. Fellous, M. Rudolph, A. Destexhe, and T. J. Sejnowski, Neuroscience **122**, 811 (2003).
[9] M. Rudolph and A. Destexhe, Phys. Rev. Lett. **86**, 3662 (2001).
[10] L. Gammaitoni, P. Hänggi, P. Jung, and F. Marchesoni, Rev. Mod. Phys. **70**, 223 (1998).
[11] K. Wiesenfeld and F. Moss, Nature (London) **373**, 33 (1995).
[12] P. Hänggi, ChemPhysChem **3**, 285 (2002).
[13] M. D. McDonnell and D. Abbott, PLOS Comput. Biol. **5**, e1000348 (2009).
[14] A. Longtin, J. Stat. Phys. **70**, 309 (1993).
[15] J. J. Collins, C. C. Chow, and T. T. Imhoff, Phys. Rev. E **52**, R3321 (1995).
[16] J. J. Collins, C. C. Chow, and T. T. Imhoff, Nature (London) **376**, 236 (1995).
[17] M. Stemmler, Network **7**, 687 (1996).
[18] B. Lindner, J. García-Ojalvo, A. Neiman, and L. Schimansky-Geier, Phys. Rep. **392**, 321 (2004).
[19] P. E. Greenwood, U. U. Müller, and L. M. Ward, Phys. Rev. E **70**, 051110 (2004).
[20] B. Kosko and S. Mitaim, Phys. Rev. E **70**, 031911 (2004).
[21] H. Yasuda, T. Miyaoka, J. Horiguchi, A. Yasuda, P. Hänggi, and Y. Yamamoto, Phys. Rev. Lett. **100**, 118103 (2008).
[22] A. Patel and B. Kosko, Neural Networks **22**, 697 (2009).
[23] X. Godivier and F. Chapeau-Blondeau, Europhys. Lett. **35**, 473 (1996).
[24] B. J. Gluckman, T. I. Netoff, E. J. Neel, W. L. Ditto, M. L. Spano, and S. J. Schiff, Phys. Rev. Lett. **77**, 4098 (1996).
[25] J. E. Levin and J. P. Miller, Nature (London) **380**, 165 (1996).
[26] D. R. Chialvo, A. Longtin, and J. Mullergerking, Phys. Rev. E **55**, 1798 (1997).
[27] N. G. Stocks and R. Mannella, Phys. Rev. E **64**, 030902(R) (2001).
[28] N. G. Stocks and R. Mannella, in *Future Directions for Intel-*

ligent Systems and Information Sciences, edited by N. Kosabov (Physica-Verlag, Heidelberg, 2000), pp. 236–247.
[29] N. G. Stocks, Phys. Rev. Lett. **84**, 2310 (2000).
[30] N. G. Stocks, Phys. Rev. E **63**, 041114 (2001).
[31] T. Hoch, G. Wenning, and K. Obermayer, Phys. Rev. E **68**, 011911 (2003).
[32] Q. S. Li and Y. Liu, Phys. Rev. E **73**, 016218 (2006).
[33] N. G. Stocks, N. D. Stein, and P. V. E. McClintock, J. Phys. A **26**, L385 (1993).
[34] S. M. Bezrukov and I. Vodyanoy, Nature (London) **385**, 319 (1997).
[35] M. Evstigneev, P. Reimann, V. Pankov, and R. H. Prince, Europhys. Lett. **65**, 7 (2004).
[36] D. Rousseau, J. Rojas Varela, and F. Chapeau-Blondeau, Phys. Rev. E **67**, 021102 (2003).
[37] F. Chapeau-Blondeau, S. Blanchard, and D. Rousseau, Phys. Rev. E **74**, 031102 (2006).
[38] F. Chapeau-Blondeau and D. Rousseau, Phys. Lett. A **351**, 231 (2006).
[39] F. Chapeau-Blondeau, F. Duan, and D. Abbott, Physica A **387**, 2394 (2008).
[40] F. Duan, F. Chapeau-Blondeau, and D. Abbott, Physica A **388**, 1345 (2009).
[41] D. Rousseau and F. Chapeau-Blondeau, Neural Process. Lett. **20**, 71 (2004).
[42] S. Blanchard, D. Rousseau, and F. Chapeau-Blondeau, Neurocomputing **71**, 333 (2007).
[43] F. Chapeau-Blondeau and N. Chambet, Neural Comput. **7**, 713 (1995).
[44] D. J. Higham, SIAM Rev. **43**, 525 (2001).
[45] M. I. Dykman, D. G. Luchinsky, R. Mannella, P. V. E. McClintock, H. E. Short, N. D. Stein, and N. G. Stocks, Phys. Lett. A **193**, 61 (1994).
[46] N. G. Stocks, N. D. Stein, H. E. Short, R. Mannella, D. G. Luchinsky, P. V. E. McClintock, and M. I. Dykman, in *Fluctuations and Order: The New Synthesis*, edited by M. Millonas (Springer, Berlin, 1993), pp. 53–67.
[47] F. Duan, F. Chapeau-Blondeau, and D. Abbott, Electron. Lett. **42**, 1008 (2006).
[48] J. M. Casado, J. Gómez Ordóñez, and M. Morillo, Phys. Rev. E **73**, 011109 (2006).
[49] F. Chapeau-Blondeau and D. Rousseau, Phys. Rev. E **70**, 060101(R) (2004).
[50] F. Duan, D. Rousseau, and F. Chapeau-Blondeau, Phys. Rev. E **69**, 011109 (2004).